REPORT DOCUMENTATION PAGE

Form Approved OMB NO. 0704-0188

1. REPORT DATE (DD-MM-YYYY)	2. REPORT TYPE	3. DATES COVERED (From - To)
31-10-2022	Final Report	1-Aug-2020 - 31-Jul-2022

4. TITLE AND SUBTITLE
Final Report: Distributed Intelligence in Kirigami-Inspired Flexible Architectures

5a. CONTRACT NUMBER
W911NF-20-1-0278

5b. GRANT NUMBER

5c. PROGRAM ELEMENT NUMBER

6. AUTHORS

5d. PROJECT NUMBER

5e. TASK NUMBER

5f. WORK UNIT NUMBER

7. PERFORMING ORGANIZATION NAMES AND ADDRESSES
University of Pennsylvania Research Servic
Office of Research Services
3451 Walnut Street Room P221 Franklin Bldg
Philadelphia, PA 19104 -6205

8. PERFORMING ORGANIZATION REPORT NUMBER

9. SPONSORING/MONITORING AGENCY NAME(S) AND ADDRESS (ES)
U.S. Army Research Office
P.O. Box 12211
Research Triangle Park, NC 27709-2211

10. SPONSOR/MONITOR'S ACRONYM(S)
ARO

11. SPONSOR/MONITOR'S REPORT NUMBER(S)
77509-ME-DRP.5

12. DISTRIBUTION AVAILIBILITY STATEMENT
Approved for public release; distribution is unlimited

13. SUPPLEMENTARY NOTES
The views, opinions and/or findings contained in this report are those of the author(s) and should not contrued as an official Department of the Army position, policy or decision, unless so designated by other documentation.

14. ABSTRACT

15. SUBJECT TERMS

16. SECURITY CLASSIFICATION OF:			17. LIMITATION OF ABSTRACT	15. NUMBER OF PAGES	19a. NAME OF RESPONSIBLE PERSON
a. REPORT	b. ABSTRACT	c. THIS PAGE			JORDAN RANEY
UU	UU	UU	UU		19b. TELEPHONE NUMBER 215-898-7106

RPPR Final Report
as of 25-Jan-2023

Agency Code: 21XD

Proposal Number: 77509MEDRP **Agreement Number: W911NF-20-1-0278**
INVESTIGATOR(S):

Name: JORDAN R RANEY
Email: raney@seas.upenn.edu
Phone Number: 2158987106
Principal: Y

Organization: **University of Pennsylvania Research Services**
Address: Office of Research Services, Philadelphia, PA 191046205
Country: USA
DUNS Number: 175373166 EIN: 231352685

Report Date: 31-Oct-2022 Date Received: 31-Oct-2022
Final Report for Period Beginning 01-Aug-2020 and Ending 31-Jul-2022
Title: Distributed Intelligence in Kirigami-Inspired Flexible Architectures
Begin Performance Period: 01-Aug-2020 **End Performance Period:** 31-Jul-2022
Report Term: 0-Other

Submitted By: JORDAN RANEY Email: raney@seas.upenn.edu
Phone: (215) 898-7106

Distribution Statement: information

STEM Degrees: 0 **STEM Participants:** 3

Major Goals: The purpose of this work is to develop a new conceptual paradigm of distributed intelligence as a material property, and to demonstrate the potential utility of this by delivering a kirigami-based robotic material capable of autonomous changes to its trajectory based on stimuli in the surrounding environment (heat, water, light, etc.).

In order to respond to their environment, most robotic systems rely on traditional mechatronic sensors that route information to a central processor, which sends subsequent commands to electronic actuators to respond to the environment. In contrast, in this work the sensing, processing, and actuating functions are spatially distributed as part of the geometry and composition itself. That is, the kirigami locally operates on, and actuates in response to, environmental inputs such as temperature, solvents, or magnetic fields, based solely on the local geometry and composition of the kirigami. The resulting local changes can be transmitted to adjacent regions via the propagation of highly nonlinear transition waves, which lead to the evolution of “phase boundaries” in the structure, and drastic changes to the morphology and mechanical properties.

To attain the above goals, we leverage a notion we refer to as embodied logic. A multimaterial direct ink writing (DIW) platform is used to 3D print a palette of materials that serve as sensors. With this single platform we are able to print silicones (to sense solvents), hydrogels (to sense water), liquid crystal elastomers (to sense temperature and light), etc. Second, we leverage the rich nonlinear and materials-independent mechanics of kirigami. We specifically design the kirigami to be multistable, based on a combination of its geometry and the use of permanent magnets embedded throughout the structure. With each kirigami unit cell supporting up to 3 stable morphologies, each unit cell is like a digital logic bit (though able to support logic states 0/1/2 instead of the traditional 0/1). Local commands can be assigned based on the composition and geometry. When the desired conditions are satisfied by the surrounding environment (temperature, solvents, light intensity, etc.), sudden local morphological changes occur (i.e., the structure locally “changes phase”). Different phases compete, affecting the total system response.

Since the logic that governs the response of the structure to its environment is embodied in the local kirigami structure and can be spatially varied, intelligence can be viewed as a material property just as strength or stiffness is. This understanding blends robotics and materials science in a potentially revolutionary paradigm. To accomplish this work, PI Raney managed a team of post-docs and PhD students for two years (year 1-2 budget total of $500k). Three Milestones were accomplished, each with growing complexity. The final deliverable was an electronics-free flexible kirigami structure capable of autonomously changing direction during locomotion based on the surrounding environment, following a simple yet powerful set of rules embodied in the structure itself (e.g., “steer away from

solvents and toward light").

Accomplishments: [See PDF for figures and additional details]

Context and project organization
The funded work was divided into four tasks (Table 1). Task 1 (Phase transforming kirigami) and Task 2 (Static analysis) culminated in Milestone A at the end of Year 1, namely, an experimental prototype demonstrating distributed logic, activated autonomously via changes to the surrounding environment. Task 3 (Proprioception) and Task 4 (Nonlinear dynamics and transition waves) culminated, at the end of year 2, in Milestone B, namely kirigami prototypes capable of sensing their own configuration. Additionally, Task 5 (Miniaturization) and Task 6 (Locomotion) were planned for optional year 3, resulting in Milestone C (Autonomous path-planning). Since year 3 was not funded, Task 5 was canceled. Nevertheless, we performed Task 6 and achieved Milestone C within the two year program, culminating in an autonomous robot that navigates its environment entirely via distributed computational events in its body, with no electronics.

Accomplishments and technical details: Milestone A
The goal of Milestone A was to experimentally build and characterize a kirigami prototype that demonstrates distributed logic. As was originally proposed, we built a 2D kirigami system with 16 different regions (in a 4x4 square pattern) capable of autonomously opening or closing in response to environmental inputs. The purpose of this was to show how spatial variations in the structure and composition of the kirigami lead to distinct localized shape changes that can be associated with different "phases", and, in an abstract sense, with information processing.

To achieve Milestone A, it was first necessary to construct several mechanisms that could be integrated with the kirigami in order to enable basic logic in response to different stimuli. Several examples of these are shown in Figure 3.

After designing mechanisms to control the localized response of different rotating units in response to their environment, such as the mechanisms shown in Fig. 3, the next step in achieving Milestone A was to combine multiple mechanisms into a single larger kirigami structure. An optical image of this structure is shown in Figure 4. Here, we produced a 2D kirigami specimen comprising 16 rotating units, each of which can be designed to respond uniquely to its surrounding environment. The dashed rectangles in Fig. 4 indicate the distinct behavior embodied in the different regions of the specimen.

In order to confirm that the structure responded to the environment as expected both locally and globally, we performed numerous experiments in which we recorded how the structure behaved when different stimuli were introduced. The relevant stimuli for this specimen include heat (sensed via LCEs), light (sensed via LCEs with embedded CNTs that converted the light to heat in the LCEs), solvents (sensed via silicones), and mechanical force (which was applied by hand). Figure 5 shows a detailed series of experiments on the specimen of Fig. 4, with these four environmental inputs being applied sequentially to different areas on the structure.

Accomplishments and technical details: Milestone B
Milestone A demonstrated the feasibility of building kirigami structures that use stimuli-responsive materials such as liquid crystal elastomers (LCEs) and hydrogels to induce autonomous structural changes in response to environmental inputs. In that work, these structural changes were observed optically. Each structural change is the result of nonlinear interactions between different parts of the kirigami, and is effectively a computational event. Different spatial configurations were associated with different information states. However, in order for a robot to autonomously make use of these different information states, it needs a different mechanism of readout (i.e., our electronics-free robots do not have optical sensors). To accomplish this, Milestone B takes inspiration from "proprioception", the ability of natural organisms to know their own structural configuration based upon internal mechanical sensors. (For example, people know where their arms are even if their eyes are closed.) Hence, in this Milestone, we aimed to associate the different structural configurations of the kirigami with different mechanical properties. A robot could then, in principle, become "aware" of its own information state based upon the property variations in its own body, enabling the robot to autonomously exhibit different behaviors as the environment influences its shape.

As the kirigami shown in Figure 5 changes shape in response to environmental stimuli, its mechanical properties also change. To characterize this effect, we built a new specimen and have experimentally and numerically measured how its static (stiffness, Poisson's ratio, etc.) and dynamic (wave propagation, response to impulse, etc.)

properties vary as a function of the spatial distribution of the phases, and the associated boundaries between the phase regions. The spatial distribution of these phases has a very large effect on both static and dynamic properties. This specimen is pictured in Figure 6. Because of its multistability, many different spatial configurations of phases can be imparted to the structure. Fig. 6 (right) shows an example of how the internal phase boundaries can alter properties, in this case, the propagation of linear waves when harmonic excitation is applied where indicated on the left boundary of the structure. These numerical simulations show that the longitudinal components of the linear waves propagate through the boundary, but that the torsional component is blocked. By measuring several static and dynamic properties for each configuration of the mechanical metamaterial, we can begin to predict what the structural configuration is solely via property changes. This inverse process (Fig. 6, bottom) is what we refer to as proprioception. Abstractly, the spatial distribution of phases represents the information state of the kirigami. Proprioception is therefore the means by which the information state can be measured.

Accomplishments and technical details: Milestone C
Though the optional third year was not funded, we were able to accelerate some of the work proposed for that year in order to achieve Milestone C in parallel with Milestone B in year 2. In this Milestone, we showed one way that abstract notions of “distributed computation” in a soft body might be applied in soft robotics. The first goal in this direction was the construction of a soft, kirigami-based, electronics-free robot that autonomously chooses its path of locomotion based on distributed “computation” in its own body. This computation occurs in response to the surrounding environmental stimuli, such as heat, light, moisture, etc. Each of these stimuli can activate or deactivate “control modules” within the kirigami body, which alter the shape and behavior of the robot. The competition of several such events steers the robot according to a high-level set of commands, such as “walk across the room but avoid sources of heat above a certain temperature”. The stimuli-responsive control units are modular. By adding, removing, or changing the location of the modules, the high-level “programming” of the robot can be altered, without any use of electronics (e.g., from “move toward light while avoiding high temperatures” to “move toward heat sources, but not if they are wet”). The combined actions of the modules constitute the entirety of the control system of the robot, which is distributed throughout the body.

Training Opportunities: PhD students and post-docs worked closely with the PI to accomplish the research tasks, including performing experiments, conducting numerical simulations, conducting theoretical and conceptual analysis, preparing technical manuscripts for publication, preparing and giving oral presentations at conferences, etc. Group meetings were conducted weekly, focusing on overall project direction and ongoing challenges. Individual meetings were also conducted weekly, i.e., between each individual student / post-doc and the PI. For those trainees departing the group, the PI also provided extensive professional mentorship, including how to write cover letters, research statements, and teaching statements, and how to successfully undertake the interview process.

The specific conference presentations and technical publications that resulted from the above activities are itemized below.

RPPR Final Report
as of 25-Jan-2023

Results Dissemination: Due to the COVID pandemic, which endured during the entire period of this project, traditional K-12 outreach and outreach to the general public were canceled. Dissemination of results therefore primarily occurred via technical publications and conference presentations. These are listed below, and in the Products section.

Publications

L. M. Korpas, R. Yin, H. Yasuda, J. R. Raney, "Temperature-responsive mechanical metamaterials," ACS Applied Materials & Interfaces 2021;13(26):31163-31170.

H. Yasuda, P. R. Buskohl, A. Gillman, T. D. Murphey, S. Stepney, R. A. Vaia, J. R. Raney, "Mechanical computing," Nature 2021;598:39-48.

Y. Miyazawa, H. Yasuda, H. Kim, J. H. Lynch, K. Tsujikawa, T. Kunimine, J. R. Raney, J. Yang, "Heterogeneous origami architected materials with variable stiffness," Communications Materials 2021;2:110.

H. Yasuda, E. G. Charalampidis, P. K. Purohit, P. G. Kevrekidis, J. R. Raney, "Wave manipulation using a bistable chain with reversible impurities," Physical Review E 2021;104:054209.

H. Yasuda, K. Johnson, V. Arroyos, K. Yamaguchi, J. R. Raney, J. Yang, "Leaf-like origami with bistability for self-adaptive grasping motion," Soft Robotics 2022 (published online, DOI: 10.1089/soro.2021.0008).

H. Yasuda, H. Shu, W. Jiao, V. Tournat, J. R. Raney, "Nucleation of transition waves via collisions of elastic vector solitons," (in review).

Q. He, R. Yin, Y. Hua, W. Jiao, C. Mo, H. Shu, J. R. Raney, "A modular strategy for distributed, embodied control of electronics-free soft robots," (in review).

Meetings and Events
•"Collision-induced phase transformations in flexible mechanical metamaterials," Symposium on Transforming (Meta-)Materials and (Meta-)Structures, SIAM annual meeting, Pittsburgh, PA, July 2022.
•"Collisions of elastic vector solitons in flexible mechanical metamaterials," Session on Metamaterials, International Symposium on Nonlinear Acoustics, Oxford, UK, July 2022.
•"Electronics-free soft robot with multi-stimuli responsive control," Symposium on Architected Materials, US National Congress on Theoretical and Applied Mechanics, Austin, TX, June 2022.
•"Collisions of nonlinear waves in flexible mechanical metamaterials," Symposium on Nonlinear Acoustic Metamaterials and Phononics, 182nd meeting of the Acoustical Society of America (ASA), Denver, CO, May 2022.
•"Electronics-free soft robot with multi-stimuli responsive control," Symposium SB03 – Robotic Materials for Advanced Machine Intelligence, Materials Research Society spring meeting, Honolulu, HI, May 2022.
•"Soft, tough, 3D-printable composites," 3M Tech Forum, Minneapolis, MN, November 2021 (virtual due to COVID).

Honors and Awards: PI Invited to Editorial Board, Programmable Materials (a new journal from Cambridge University Press), 2022

PI Invited to Editorial Board, Communications Engineering, a Nature family journal, 2021

Protocol Activity Status:

Technology Transfer: "Electronics-free control method for compliant robots," Q. He, R. Yin, Y. Hua, W. Jiao, C. Mo, H. Shu, J. R. Raney, provisional patent filed (2/23/2022), US Provisional No.: 63/313,013.

PARTICIPANTS:

Participant Type: PD/PI
Participant: Jordan Raney
Person Months Worked: 2.00 **Funding Support:**
Project Contribution:

National Academy Member: N

Participant Type: Postdoctoral (scholar, fellow or other postdoctoral position)
Participant: Weijian Jiao
Person Months Worked: 6.00 **Funding Support:**
Project Contribution:
National Academy Member: N

Participant Type: Postdoctoral (scholar, fellow or other postdoctoral position)
Participant: Qiguang He
Person Months Worked: 15.00 **Funding Support:**
Project Contribution:
National Academy Member: N

Participant Type: Postdoctoral (scholar, fellow or other postdoctoral position)
Participant: Hiromi Yasuda
Person Months Worked: 3.00 **Funding Support:**
Project Contribution:
National Academy Member: N

Participant Type: Graduate Student (research assistant)
Participant: Hang Shu
Person Months Worked: 4.00 **Funding Support:**
Project Contribution:
National Academy Member: N

Participant Type: Graduate Student (research assistant)
Participant: Saheli Patel
Person Months Worked: 4.00 **Funding Support:**
Project Contribution:
National Academy Member: N

Participant Type: Graduate Student (research assistant)
Participant: Yucong Hua
Person Months Worked: 4.00 **Funding Support:**
Project Contribution:
National Academy Member: N

RPPR Final Report
as of 25-Jan-2023

Partners

,

I certify that the information in the report is complete and accurate:
Signature: Jordan R. Raney
Signature Date: 10/31/22 2:24PM

Jordan R. Raney, University of Pennsylvania
DARPA DSO
Grant #W911NF2010278
Final Report

Period Covered by the Report
August 1, 2020 through July 31, 2022

Date of Report: October 31, 2022

Project Title: Distributed Intelligence in Kirigami-Inspired Flexible Architectures
Total Dollar Value: 500,000
Program Managers: Rohith Chandrasekar, Jiangying Zhou, Dean Culver

Submitted by:
Jordan R. Raney
Towne Building Rm 274
220 S. 33rd St.
Philadelphia, PA 19104-6315
Telephone: 215-573-9928
Fax: 215-573-9928
Email: raney@seas.upenn.edu

Distribution List and Addresses
Rohith Chandrasekar (rohith.chandrasekar@darpa.mil), Jiangying Zhou (jiangying.zhou@darpa.mil), Dean Culver (dean.r.culver.civ@mail.mil), Grace Rigdon (Grace.Rigdon.ctr@darpa.mil)

Security Classification – Unclassified

Technical & Financial Summary

1. **Technical Progress / Expenditure Report (Please provide cumulative spending graph).**

Figure 1 shows project spending with monthly resolution. The project ran from August 1, 2020 through July 31, 2022, with a total budget of $500,000. The project milestones were completed, along with total funding expenditures, on schedule. There were a few notable months of underspending (primarily Q3-4) and overspending (primarily Q5-6) due to personnel changes.

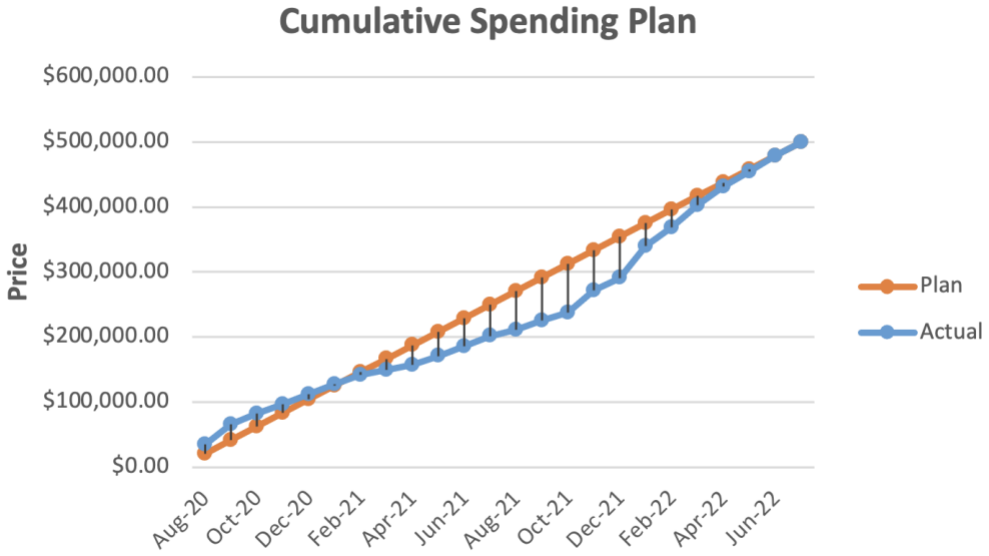

Figure 1. Cumulative spending plan.

2. **Technical Progress:**

Project executive summary

The purpose of this work is to develop a new conceptual paradigm of *distributed intelligence as a material property*, and to demonstrate the potential utility of this by delivering a kirigami-based robotic material capable of autonomous changes to its trajectory based on stimuli in the surrounding environment (heat, water, light, etc.).

In order to respond to their environment, most robotic systems rely on traditional mechatronic sensors that route information to a central processor, which sends subsequent commands to electronic actuators to respond to the environment. In contrast, in this work the sensing, processing, and actuating functions are spatially distributed as part of the geometry and composition itself. That is, the kirigami locally operates on, and actuates in response to, environmental inputs such as temperature, solvents, or magnetic fields, based solely on the local geometry and composition of the kirigami. The resulting local changes can be transmitted to

adjacent regions via the propagation of highly nonlinear transition waves, which lead to the evolution of "phase boundaries" in the structure, and drastic changes to the morphology and mechanical properties.

To attain the above goals, we leverage a notion we refer to as embodied logic. A multimaterial direct ink writing (DIW) platform is used to 3D print a palette of materials that serve as sensors. With this single platform we are able to print silicones (to sense solvents), hydrogels (to sense water), liquid crystal elastomers (to sense temperature and light), etc. Second, we leverage the rich nonlinear and materials-independent mechanics of kirigami. We specifically design the kirigami to be multistable, based on a combination of its geometry and the use of permanent magnets embedded throughout the structure. With each kirigami unit cell supporting up to 3 stable morphologies, each unit cell is like a digital logic bit (though able to support logic states 0/1/2 instead of the traditional 0/1). Local commands can be assigned based on the composition and geometry. When the desired conditions are satisfied by the surrounding environment (temperature, solvents, light intensity, etc.), sudden local morphological changes occur (i.e., the structure locally "changes phase"). Different phases compete, affecting the total system response (see **Figure 2**).

Since the logic that governs the response of the structure to its environment is embodied in the local kirigami structure and can be spatially varied, intelligence can be viewed as a material property just as strength or stiffness is. This understanding blends robotics and materials science in a potentially revolutionary paradigm. To accomplish this work, PI Raney managed a team of one post-doc and one PhD student for two years (year 1-2 budget total of $500k). Three Milestones were accomplished, each with growing complexity. The final deliverable was an electronics-free flexible kirigami structure capable of autonomously changing direction during locomotion based on the surrounding environment, following a simple yet powerful set of rules embodied in the structure itself (e.g., "steer away from solvents and toward light").

Table 1: Project schedule (from the original research proposal).

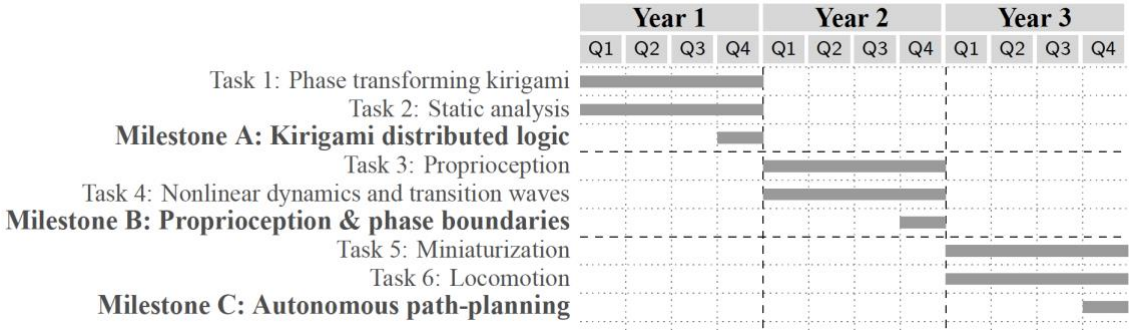

Context and project organization

The funded work was divided into four tasks (Table 1). Task 1 (Phase transforming kirigami) and Task 2 (Static analysis) culminated in Milestone A at the end of Year 1, namely, an experimental prototype demonstrating distributed logic, activated autonomously via changes to the surrounding environment. Task 3 (Proprioception) and Task 4 (Nonlinear dynamics and transition waves) culminated, at the end of year 2, in Milestone B, namely kirigami prototypes capable of sensing their own configuration. Additionally, Task 5 (Miniaturization) and Task 6 (Locomotion) were planned for optional year 3, resulting in Milestone C (Autonomous path-

planning). Since year 3 was not funded, Task 5 was canceled. Nevertheless, we performed Task 6 and achieved Milestone C within the two year program, culminating in an autonomous robot that navigates its environment entirely via distributed computational events in its body, with no electronics.

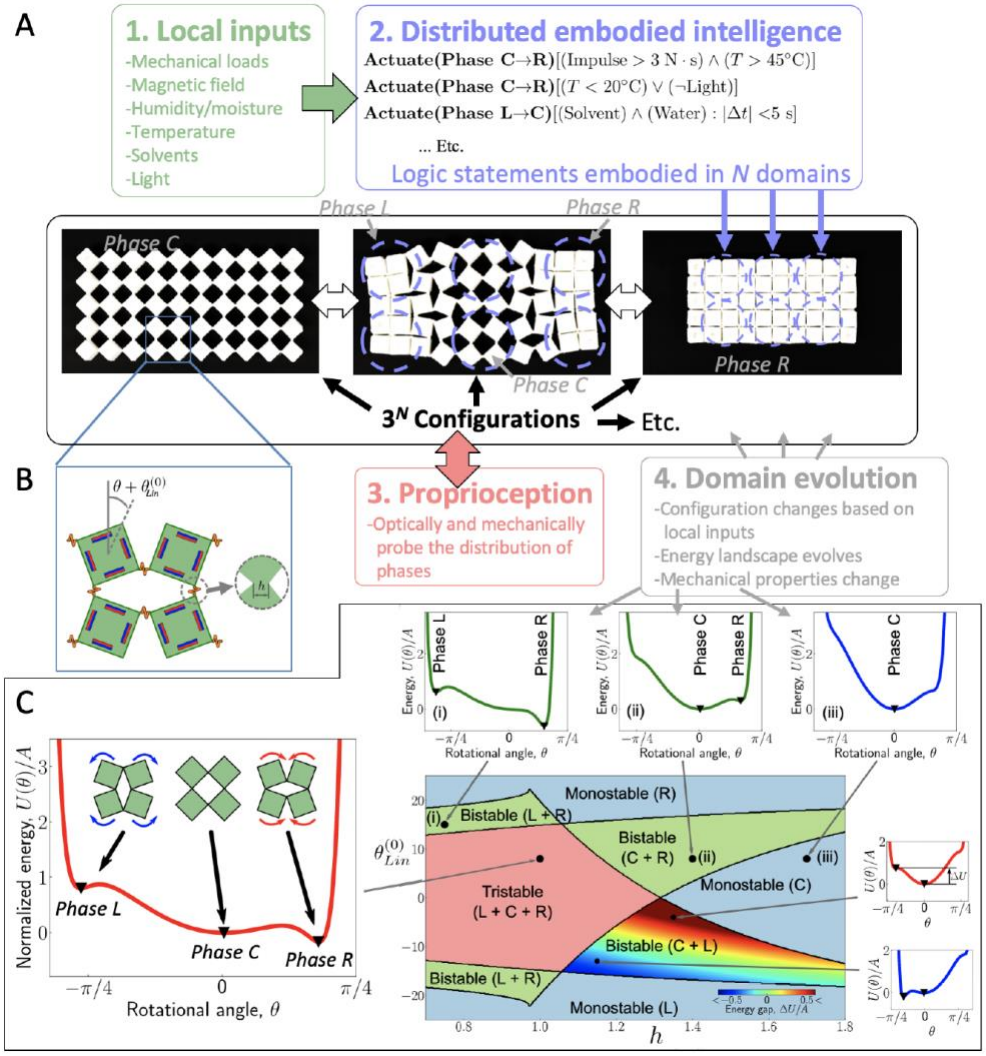

Figure 2. Overview. (A) Basic scheme: (1) Stimuli in the environment (heat, light, etc.) interact with the local kirigami structure. (2) Multistable kirigami structures are fabricated from multiple materials, each designed to respond to different stimuli. The local composition and geometry of the kirigami act as distributed intelligence, determining the "commands" and logic dictating how the kirigami locally responds to its environment (producing local "phase changes"). (3) The results of the distributed logical operations can be ascertained via optical or mechanical proprioception of the entire structure. (4) Based on continued environmental inputs and the intrinsic nonlinear dynamics of the kirigami, the phases can continue to evolve, altering the static and dynamic properties of the structure (e.g., Phase C is very flexible, while Phases R and L are much more rigid). (B) Each unit cell is modeled as a set of rigid squares connected by flexible hinges *h*. Embedded magnets enable multistability. (C) Geometric "phase diagram". The environmental inputs cause *h* and the angle of zero strain energy to vary with time, crossing phase boundaries that drastically alter the energy landscape, the distribution of phases in the kirigami, and the mechanical behavior.

Accomplishments and technical details: Milestone A

The goal of Milestone A was to experimentally build and characterize a kirigami prototype that demonstrates distributed logic. As was originally proposed, we built a 2D kirigami system with 16 different regions (in a 4x4 square pattern) capable of autonomously opening or closing in response to environmental inputs. The purpose of this was to show how spatial variations in the structure and composition of the kirigami lead to distinct localized shape changes that can be associated with different "phases", and, in an abstract sense, with information processing.

To achieve Milestone A, it was first necessary to construct several mechanisms that could be integrated with the kirigami in order to enable basic logic in response to different stimuli. Several examples of these are shown in **Figure 3**. For example, Fig. 3a shows how a liquid crystal elastomer (LCE) can be integrated with kirigami to enable a change in phase (in this case, from a *closed* to an *open* state) when the temperature in the surrounding environment increases. Fig. 3b-c show two different kinds of logical OR gates, which can trigger either an *opening* (Fig. 3b) or *closing* (Fig. 3c) of the kirigami, depending on the placement of an LCE strip with embedded carbon nanotubes (LCEs), which convert light to heat to actuate the LCE. A logical AND gate can be achieved as shown in Fig. 3d, which requires both heat and light to be present to initiate a phase change. In these examples we used variations of LCEs, but these materials could be replaced by other materials that respond to some other input from the environment. For example, if hydrogels are used, it would be the level of moisture in the environment that would determine the phase of the kirigami rather than the temperature. The use of other materials and more complex mechanisms can lead to other logic, as we have explored at a basic level in previous work.[1]

After designing mechanisms to control the localized response of different rotating units in response to their environment, such as the mechanisms shown in Fig. 3, the next step in achieving Milestone A was to combine multiple mechanisms into a single larger kirigami structure. An optical image of this structure is shown in **Figure 4**. Here, we produced a 2D kirigami specimen comprising 16 rotating units, each of which can be designed to respond uniquely to its surrounding environment. The dashed rectangles in Fig. 4 indicate the distinct behavior embodied in the different regions of the specimen.

[1] Y. Jiang, L. M. Korpas, J. R. Raney, "Bifurcation-based embodied logic and autonomous actuation," Nature Communications 2019;10:128.

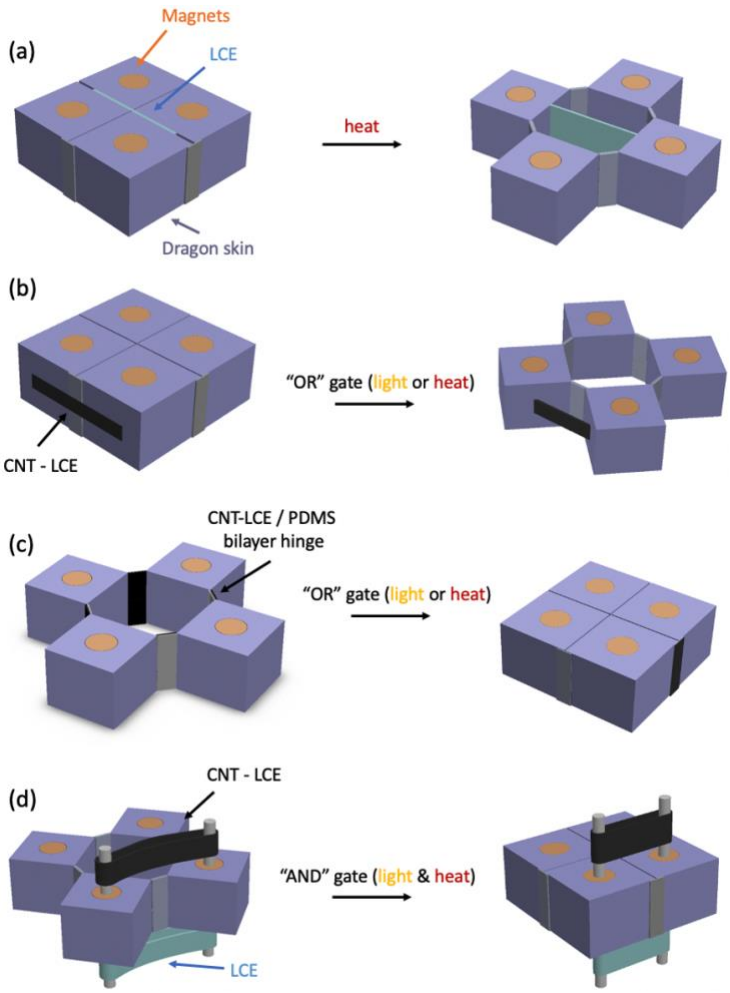

Figure 3. Schematics of several example mechanisms designed for this work. (a) An LCE strip placed from the inside face of one square to the inside face of another square causes the squares to *open* when heat is applied. (b) If CNTs are added to the LCE, which absorb light to create local heating, an OR gate can be constructed that *opens* in the presence of either heat or light. (c) If instead the CNT-LCE strips are incorporated as bilayer hinges, an OR gate can be constructed that *closes* in the presence of either heat or light. (d) If CNT-LCE and LCE strips are arranged as shown, an AND gate can be constructed that closes only if both heat and light are applied.

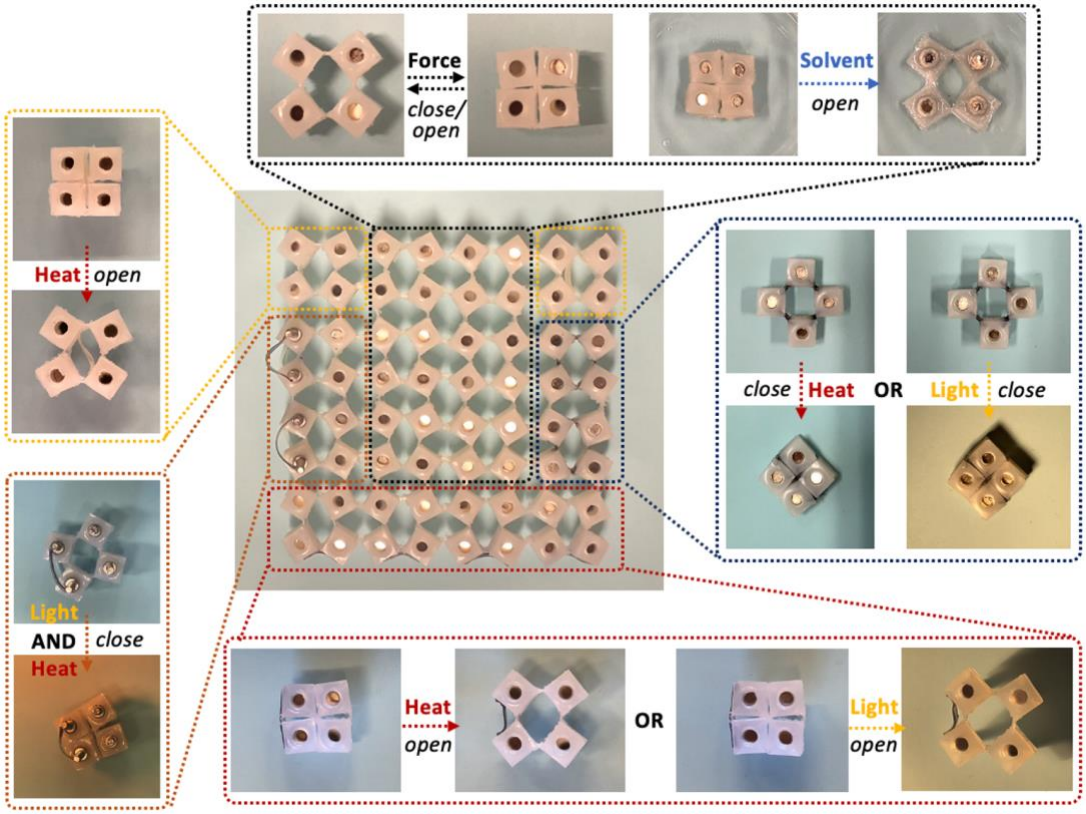

Figure 4. An optical image of a specimen comprising 16 rotating units, each of which could be designed with a different mechanism (see, e.g., Fig. 1) and with different materials to enable autonomous shape change and information processing in response to different cues from the environment. The dashed rectangles indicate the types of mechanisms used in different regions of the specimen.

In order to confirm that the structure responded to the environment as expected both locally and globally, we performed numerous experiments in which we recorded how the structure behaved when different stimuli were introduced. The relevant stimuli for this specimen include *heat* (sensed via LCEs), *light* (sensed via LCEs with embedded CNTs that converted the light to heat in the LCEs), *solvents* (sensed via silicones), and *mechanical force* (which was applied by hand). **Figure 5** shows a detailed series of experiments on the specimen of Fig. 4, with these four environmental inputs being applied sequentially to different areas on the structure. Initially, all units are set to the *open* phase (configuration 1 in Fig. 5). Based on the spatial distribution of the different mechanisms and associated materials types, the introduction of different stimuli can lead to the same or very different spatial configurations of the kirigami. For example, if light is applied to the entire structure when it is in configuration 1, only the right side actuates to a *closed* phase (configuration 2(1)). This is because the right side of the specimen consists of OR gates that close in response to heat or light. (Note, there is also an OR gate along the bottom of the structure that would cause the structure to *open* in response to heat or light, but since this area is already in an *open* state in configuration 1 the bottom of the structure does not change.) Because it is an OR gate, the same configuration (configuration 2(2)) can be achieved by application of heat instead. Subsequently, configuration 3 can be achieved by applying both heat and light to the left side (this region is an AND gate that only actuates if both heat and light are applied). Next, configuration 4 is achieved by applying mechanical force to transition the entire structure to the closed state. Configurations 5-7 are achieved by sequential application of

localized light or heat. Finally, configuration 8 is reached via global application of solvent, which causes the silicone to swell and prefer an open state. Configuration 8 is also an example in which different phases in different regions are in competition.

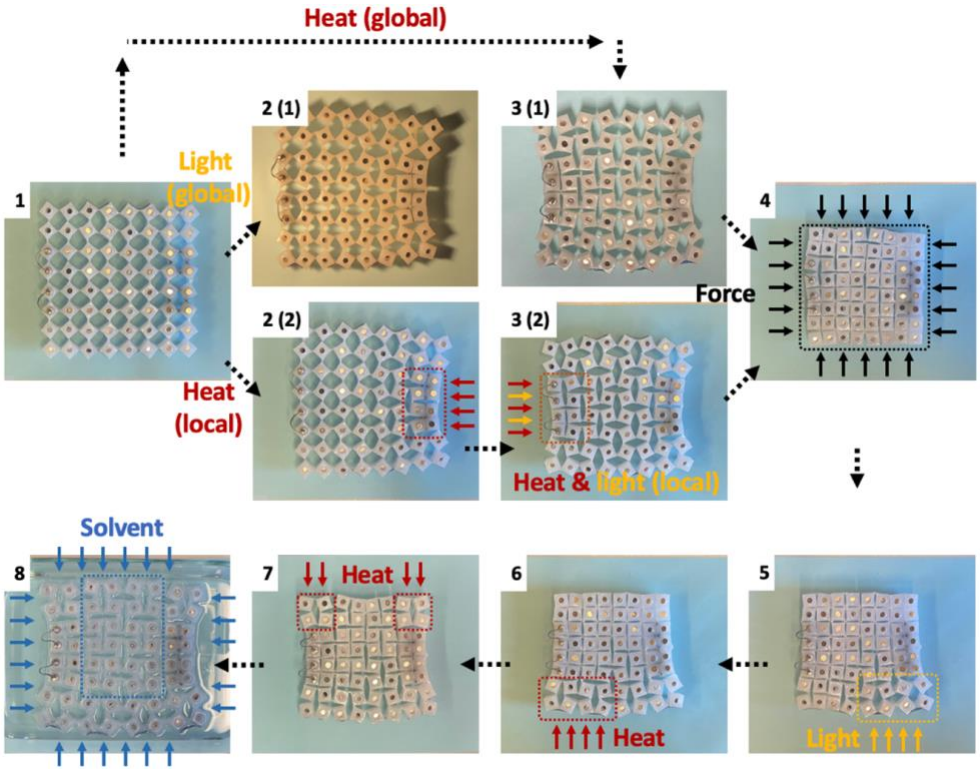

Figure 5. In the initial configuration 1 all units are in the *open* phase. Starting from this configuration, it is immediately evident that distinct applications of environmental stimuli might lead to the same state. For example, configuration 2(1) and 2(2) are identical. Configuration 2(1), in which the right edge folds into a *closed* phase, was achieved by application of light to the entire structure. As shown in Fig. 2, this region consists of an OR gate of heat or light, hence the same configuration can be achieved via local application of heat (i.e., configuration 2(2)). Subsequently, configuration 3 can be achieved by applying both heat and light to the left side (this region is an AND gate that requires both inputs to actuate, as shown in Fig. 2). Next, configuration 4 is achieved by applying mechanical force to transition the entire structure to the *closed* state. Configurations 5-7 are achieved by sequential application of localized light or heat. Finally, configuration 8 is reached via global application of solvent, which causes the silicone to swell and prefer an *open* state.

Accomplishments and technical details: Milestone B

Milestone A demonstrated the feasibility of building kirigami structures that use stimuli-responsive materials such as liquid crystal elastomers (LCEs) and hydrogels to induce autonomous structural changes in response to environmental inputs. In that work, these structural changes were observed optically. Each structural change is the result of nonlinear interactions between different parts of the kirigami, and is effectively a computational event. Different spatial configurations were associated with different information states. However, in order for a robot to autonomously make use of these different information states, it needs a different mechanism of readout (i.e., our electronics-free robots do not have optical sensors). To accomplish this, Milestone B takes inspiration from “proprioception”, the ability of natural organisms to know their own structural configuration based upon internal mechanical sensors. (For example, people

know where their arms are even if their eyes are closed.) Hence, in this Milestone, we aimed to associate the different structural configurations of the kirigami with different mechanical properties. A robot could then, in principle, become "aware" of its own information state based upon the property variations in its own body, enabling the robot to autonomously exhibit different behaviors as the environment influences its shape.

As the kirigami shown in Figure 5 changes shape in response to environmental stimuli, its *mechanical properties* also change. To characterize this effect, we built a new specimen and have experimentally and numerically measured how its static (stiffness, Poisson's ratio, etc.) and dynamic (wave propagation, response to impulse, etc.) properties vary as a function of the spatial distribution of the phases, and the associated boundaries between the phase regions. The spatial distribution of these phases has a very large effect on both static and dynamic properties. This specimen is pictured in **Figure 6**. Because of its multistability, many different spatial configurations of phases can be imparted to the structure. Fig. 6 (right) shows an example of how the internal phase boundaries can alter properties, in this case, the propagation of linear waves when harmonic excitation is applied where indicated on the left boundary of the structure. These numerical simulations show that the longitudinal components of the linear waves propagate through the boundary, but that the torsional component is blocked. By measuring several static and dynamic properties for each configuration of the mechanical metamaterial, we can begin to predict what the structural configuration is solely via property changes. This inverse process (Fig. 6, bottom) is what we refer to as *proprioception*. Abstractly, the spatial distribution of phases represents the information state of the kirigami. Proprioception is therefore the means by which the information state can be measured.

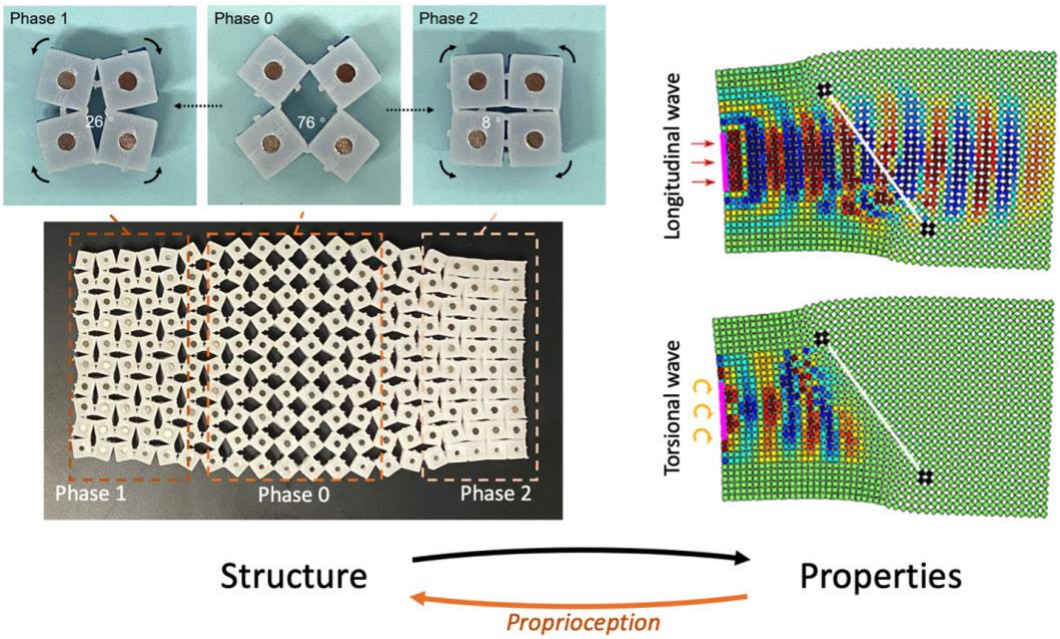

Figure 6. (Left) The kirigami is capable of many stable conformations due to the multistability of the individual units. Each unit is capable of three "phases"; the spatial distribution of these phases, and the associated *interfaces* between phase regions, defines the *structure* of the metamaterial. (Right) The spatial distribution of phases and phase boundaries has a large effect on the static and dynamic mechanical properties, such as, shown here, the ability of different types of waves to propagate through the structure.

Accomplishments and technical details: Milestone C

Though the optional third year was not funded, we were able to accelerate some of the work proposed for that year in order to achieve Milestone C in parallel with Milestone B in year 2. In this Milestone, we showed one way that abstract notions of "distributed computation" in a soft body might be applied in soft robotics. The first goal in this direction was the construction of a soft, kirigami-based, electronics-free robot that autonomously chooses its path of locomotion based on distributed "computation" in its own body. This computation occurs in response to the surrounding environmental stimuli, such as heat, light, moisture, etc. Each of these stimuli can activate or deactivate "control modules" within the kirigami body, which alter the shape and behavior of the robot. The competition of several such events steers the robot according to a high-level set of commands, such as "walk across the room but avoid sources of heat above a certain temperature". The stimuli-responsive control units are modular. By adding, removing, or changing the location of the modules, the high-level "programming" of the robot can be altered, without any use of electronics (e.g., from "move toward light while avoiding high temperatures" to "move toward heat sources, but not if they are wet"). The combined actions of the modules constitute the entirety of the control system of the robot, which is distributed throughout the body.

Our basic robot design is shown in **Figure 7**. The primary structure is the same "rotating-squares" kirigami mechanism that we have already studied extensively. However, in this case the kirigami is engineered to be stable in the closed state (as pictured in Figure 7). A pneumatic actuator is placed between two kirigami layers. When air pressure is applied to the actuator it extends longitudinally, causing the kirigami to open. Since the kirigami is only stable in its closed state, as soon as the pressure is removed the kirigami squares rotate inward and the kirigami returns to its closed configuration. Small feet placed under the bottom kirigami layer allows this extension-contraction cycle to produce locomotion. The final component of the robot is a collection of control modules which, like legos, can be easily added or removed at arbitrary locations in the robot. These will be discussed in more detail below.

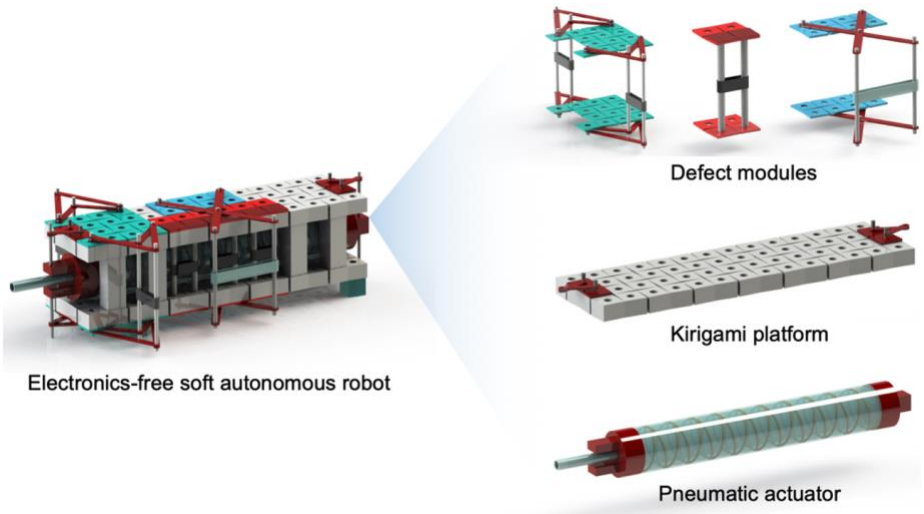

Figure 7. The kirigami soft robot consists of three primary layers: (1) a pneumatic actuator, which enables locomotion; (2) the kirigami, or "structural", layers, which provide mechanical support and act as attachment points for defects; and (3) defect modules (or "control modules"), which plug into the kirigami layers to manipulate their deformation, and, hence, the conformation and locomotion path of the robot.

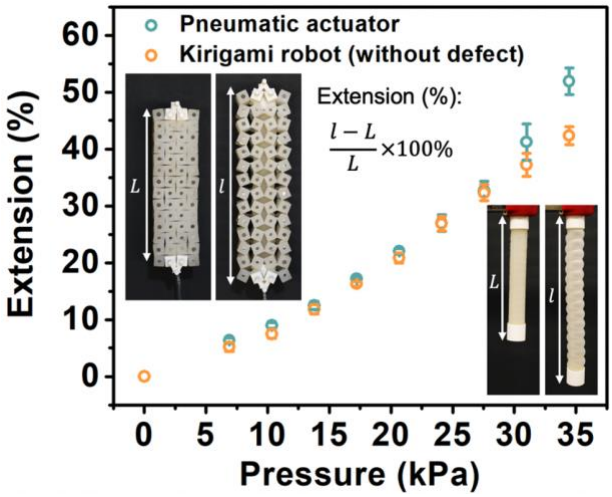

Figure 8. We have characterized the extension of the pneumatic actuator as a function of applied air pressure, both when it is integrated with the kirigami robot and when it is separate. The minor discrepancy at higher pressures occurs due to buckling of the pneumatic actuator (arising from the compressive forces that result from the interactions with the kirigami).

First, we characterized the effect of the pneumatic actuator by itself, and then on the deformation of the kirigami system when no defects are present. As shown in **Figure 8**, the kirigami can be extended by 35-40% via the pneumatic actuator at modest pressures (approximately 30 kPa). Because the kirigami is so compliant, the pneumatic actuator behaves roughly the same regardless of the presence of kirigami. Only at the highest extensions is there some discrepancy, as the pneumatic actuator can begin to buckle due to the axial load (due to the compressive forces that arise in the actuator as it expands the kirigami).

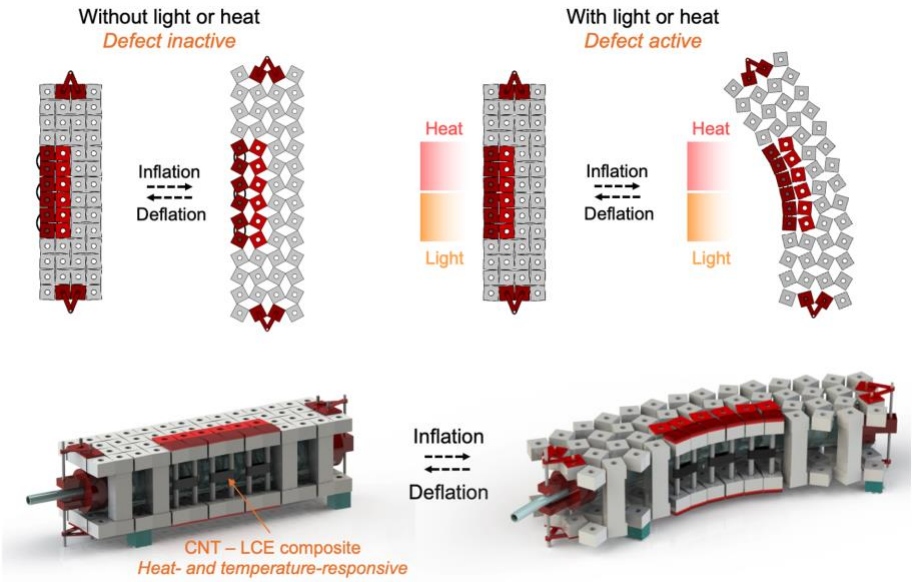

Figure 9. Because the kirigami is compliant, only small forces are required to affect the deformation of the structure. Defects, or "control modules (indicated by red squares), are activated or deactivated via interaction with the environment (heat or light, in this figure). These influences cause the kirigami to bend when it is inflated by the pneumatic actuator, causing the robot to turn.

Figure 9 shows the basic mechanism by which the control modules (or "defects") can be activated by stimuli, and how this affects the shape (and, therefore, trajectory) of the robot. In this example, the defects are controlled by liquid crystal elastomers (LCEs) with embedded carbon nanotubes (CNTs). The LCEs contract when their temperature increases. Since CNTs can warm significantly as they absorb light, the CNTs enable the LCEs to also contract in response to light. In the example in Figure 8, the CNT-LCE composite is placed along one side of the robot. When light or heat impinge on this side of the robot, it curves in that direction, causing the robot to steer in the direction of the heat/light stimulus. Of course, the contraction of the CNT-LCE composite is a function of how much heat or light is impinging on it. In **Figure 10** we quantify this relationship by experimentally measuring the bending angle of the robot as a function of the distance *d* between the stimulus source and the robot and of the pressure in the pneumatic actuator. Figure 10(a) and Figure 10(b) show the bending angle of the robot when subjected to light and heat, respectively. The schematic in Figure 10(c) and the experimental images in Figure 10(d) show how this curvature change affects the robot trajectory. In this case, a modular defect was designed that bends the trajectory toward the stimulus (light). Similarly, Figure 10(e-f) show a schematic and experimental images demonstrating how defects can also be designed that bend the trajectory away from a stimulus (heat, in this case).

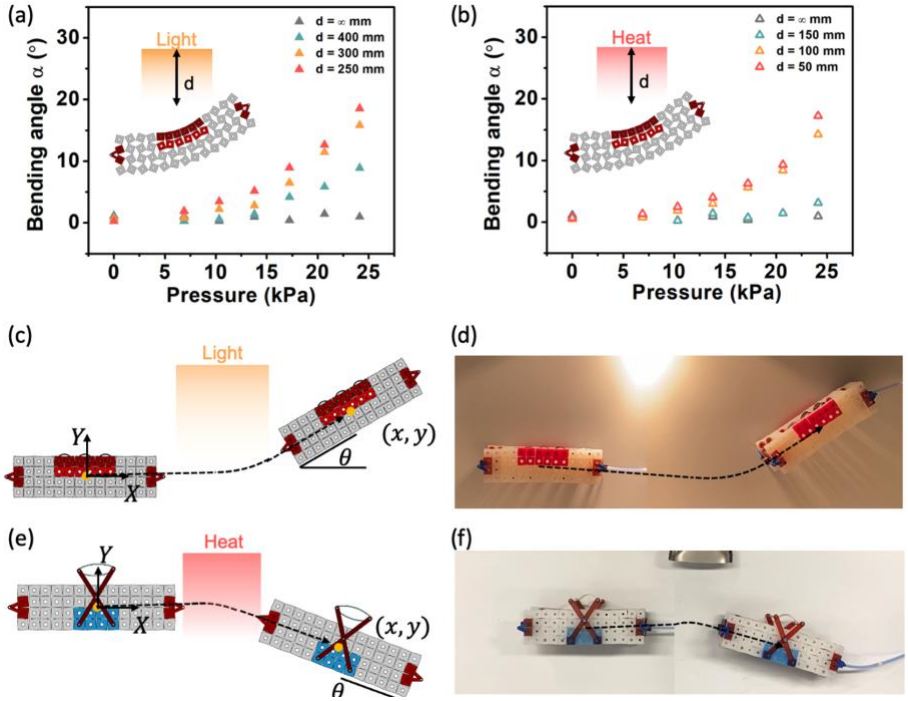

Figure 10. The amount of heat or light received by the defects of Figure 7 will determine to what degree the CNT-LCE composite contracts. (a) The effect of light exposure on the bending angle of the robot, as a function of the distance between light source and robot (*d*) and of the pressure in the pneumatic actuator; (b) the same data but now as a function of distance between heat source and robot (*d*); (c-d) a schematic and experimental images, respectively, showing how a defect can be designed that causes the trajectory of the robot to bend toward a stimulus (in this case, light); (e-f) a schematic and experimental images, respectively, showing how a defect can be designed that causes the trajectory of the robot to bend away from a stimulus (in this case, heat).

The experiments in Figure 10 demonstrate the feasibility of our basic idea, i.e., of *embodying the control system* in the robot itself, making use of modular defects to determine how the robot responds to its environment rather than any electronics. In fact, many other types of defects can be envisioned beyond those demonstrated in Figure 10. **Figure 11** shows a conceptual sketch of different defect types. More intriguingly, we can also combine multiple defects within the structure to produce competing effects. These defects could be designed to respond to the same or to different stimuli in the environment, depending on the desired functionality (e.g., the same defects shown in Figure 10 could be fabricated from hydrogels instead of LCEs, which would impart functionality in response to moisture changes rather than to heat/light). One of the key points to keep in mind is that *the defects are modular and easily added/removed*. Since the defects are responsible for determining the behavior of the robot, the distributed defects *constitute* the control system. There is no separate electronic control system. The user of the robot would determine the desired high-level behavior (e.g., "move toward light while avoiding moisture") and select the defects that would impart that functionality. The body of the robot would then compute an appropriate trajectory based on the distributed structure and defects within the robot itself. **Figure 12** provides an example of how we characterize the action of a control module and its effect on the bending angle of the robot. In this case, the robot head is autonomously directed toward heat or light, causing the robot to steer toward these stimuli.

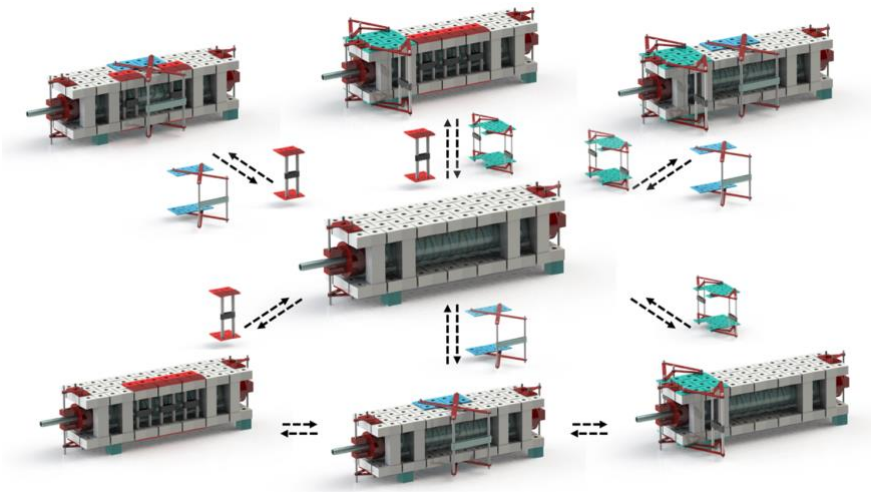

Figure 11. We have designed many types of defects, capable of steering the robot toward or away from various stimuli. Multiple defects can also be combined to produce a more complex response.

Finally, we have begun to quantify the effect of multiple defects. **Figure 13** shows one simple example of the complexities that can arise when multiple defects are used in a robot. In this case, two defects, which can be individually activated, are placed on opposite sides of the robot. If neither or both of these are active, the robot has zero curvature and moves directly forward when pneumatically actuated. If only one of the defects is active, the robot will have non-zero curvature (which can be either positive or negative, depending on which defect is active). As shown in Figure 13, this allows us to construct a *truth table* that captures the *distributed logic* embodied in the robot/defect structure. Such truth tables are used in discrete mathematics and logic to describe the outputs of logic gates (AND, OR, XOR, etc.) as a function of all possible inputs. Our truth tables are analogous to these, but quickly grow quite complex. For example, they can include a large number of inputs (a function of the number of defects and their spatial

distribution). **Figure 14** shows the experimental characterization of a NOR gate. We have similar data for XOR, OR, and AND behaviors.

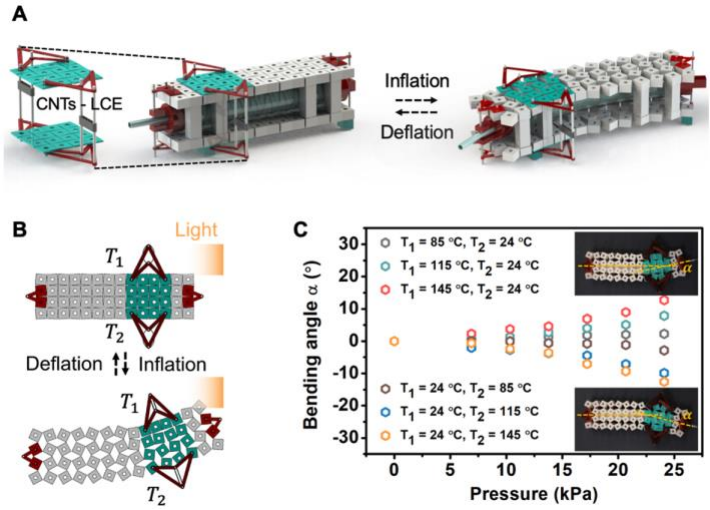

Figure 12. Experimental measurements of a control module designed to steer the robot toward a stimulus. Here we measure the temperatures T_1 and T_2 on the two sides of the module when it is subject to different amounts and locations of light. We relate this to the resulting bending angle of the robot.

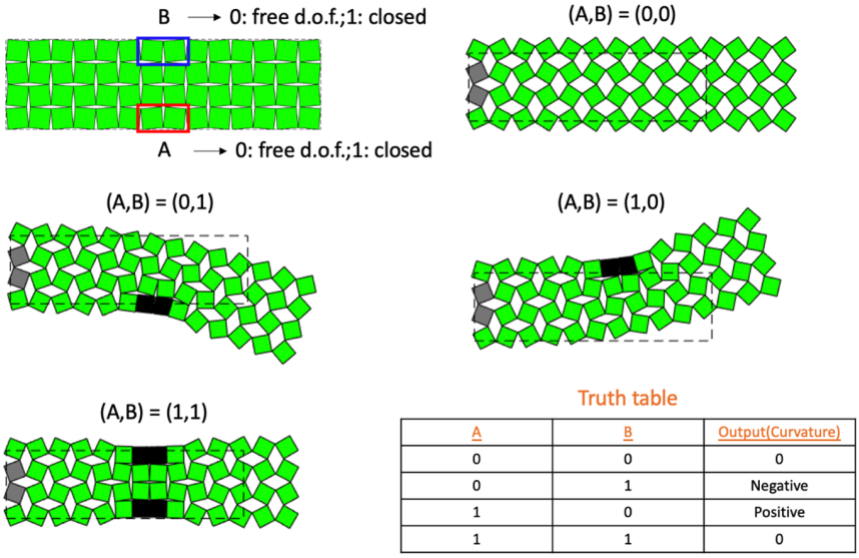

Truth table

A	B	Output(Curvature)
0	0	0
0	1	Negative
1	0	Positive
1	1	0

Figure 13. Combining multiple defects can lead to distributed logic; this means that the body of the robot will have different conformations depending upon the evaluation of multiple, distributed defects. In this example, two defects, *A* and *B* can be independently activated on the two opposite sides of the kirigami robot. If neither is activated (A,B) = (0,0) or if both are activated (A,B) = (1,1) the robot curvature remains zero, and the trajectory of the robot proceeds directly forward. If only one of the defects is activated the robot will have non-zero curvature (either positive or negative, depending on which defect is active).

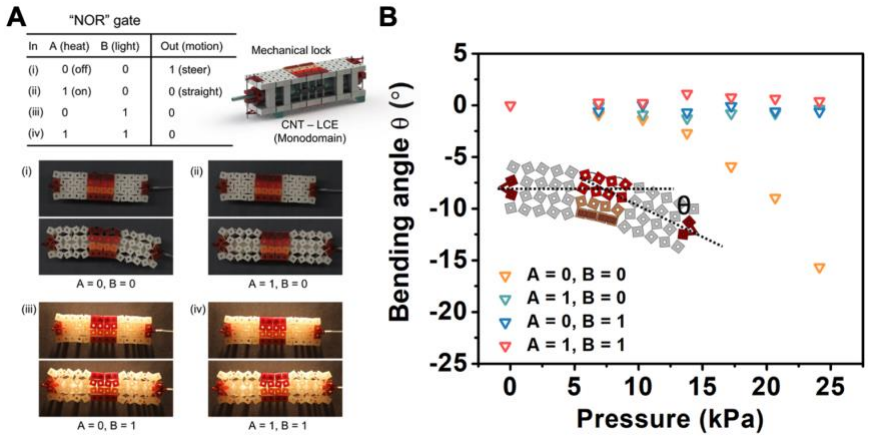

Figure 14. Two modules A and B can be used to realize a NOR behavior for the trajectory of the robot.

3. Publications (relevant to effort)

L. M. Korpas, R. Yin, H. Yasuda, J. R. Raney, "Temperature-responsive mechanical metamaterials," ACS Applied Materials & Interfaces 2021;*13*(26):31163-31170.

H. Yasuda, P. R. Buskohl, A. Gillman, T. D. Murphey, S. Stepney, R. A. Vaia, J. R. Raney, "Mechanical computing," Nature 2021;*598*:39-48.

Y. Miyazawa, H. Yasuda, H. Kim, J. H. Lynch, K. Tsujikawa, T. Kunimine, J. R. Raney, J. Yang, "Heterogeneous origami architected materials with variable stiffness," Communications Materials 2021;*2*:110.

H. Yasuda, E. G. Charalampidis, P. K. Purohit, P. G. Kevrekidis, J. R. Raney, "Wave manipulation using a bistable chain with reversible impurities," Physical Review E 2021;*104*:054209.

H. Yasuda, K. Johnson, V. Arroyos, K. Yamaguchi, J. R. Raney, J. Yang, "Leaf-like origami with bistability for self-adaptive grasping motion," Soft Robotics 2022 (published online, DOI: 10.1089/soro.2021.0008).

H. Yasuda, H. Shu, W. Jiao, V. Tournat, J. R. Raney, "Nucleation of transition waves via collisions of elastic vector solitons," (in review).

Q. He, R. Yin, Y. Hua, W. Jiao, C. Mo, H. Shu, J. R. Raney, "A modular strategy for distributed, embodied control of electronics-free soft robots," (in review).

4. Meetings and Events (please include meetings with subcontractors if applicable)

•"Collision-induced phase transformations in flexible mechanical metamaterials," Symposium on Transforming (Meta-)Materials and (Meta-)Structures, SIAM annual meeting, Pittsburgh, PA, July 2022.
•"Collisions of elastic vector solitons in flexible mechanical metamaterials," Session on Metamaterials, International Symposium on Nonlinear Acoustics, Oxford, UK, July 2022.
•"Electronics-free soft robot with multi-stimuli responsive control," Symposium on Architected Materials, US National Congress on Theoretical and Applied Mechanics, Austin, TX, June 2022.

•“Collisions of nonlinear waves in flexible mechanical metamaterials,” Symposium on Nonlinear Acoustic Metamaterials and Phononics, 182nd meeting of the Acoustical Society of America (ASA), Denver, CO, May 2022.
•“Electronics-free soft robot with multi-stimuli responsive control,” Symposium SB03 – Robotic Materials for Advanced Machine Intelligence, Materials Research Society spring meeting, Honolulu, HI, May 2022.
•“Soft, tough, 3D-printable composites,” 3M Tech Forum, Minneapolis, MN, November 2021 (virtual due to COVID).

5. Other

N/A